SANDPILE MODELLING OF PELLET PACING IN FUSION PLASMAS

C. A. BOWIE
Australian National University
Canberra, Australia
Email: craig.bowie@anu.edu.au

M. J. HOLE
Australian National University
Canberra, Australia

Abstract

Sandpile models have been used to provide simple phenomenological models without incorporating the detailed features of a fully featured model. The Chapman sandpile model (Chapman *et al Physical Review Letters* 86, 2814 (2001)) has been used as an analogue for the behaviour of a plasma edge, with mass loss events (MLEs) being used as analogues for (and anagrams of) ELMs. Here we modify the Chapman sandpile model to form comparisons with pellet pacing, which is used to reduce or eliminate ELMs. We use two different versions of the Chapman model, one in which the system is allowed to relax following an avalanche before further sand (*dx*) is added (classic model), and one in which further sand is added while an avalanche is propagating (running model). For this purpose, we modify the models in two different ways. First, we increase the amount of sand added at each time step, so that we move from the low driving model typically used in sandpile modelling to a high driving model. Second, we add 'bursts' of sand at intervals which are synchronised to MLEs in the sandpile, by way of comparison with pellet injection in a fusion plasma. We then analyse the behaviour of the sandpile in these new models, focusing on changes in the total system size, and on the maximum MLE size (by way of analogy with maximum ELM size). We observe that at low *dx*, potential energy (E_p) varies with *dx* in the running model, while *Ep* remains constant in the classic model. Analysis of *Ep/Ep max* against *dx/Zc* for increasing *dx* shows that step changes occur, often at integer ratios. An heuristic explanation is suggested for this behaviour.

1. INTRODUCTION

Pellet injection has been extensively used as a candidate for ELM control and reduction in fusion plasmas.[1-10]Pellet size, frequency, and location have all been tested experimentally on ASDEX Upgrade[6, 8, 11], DIII-D[2, 4], JET[5, 8, 12], and EAST[13, 14] and ELM control using pellets is being considered for use in ITER[5, 15].

One way of addressing the impact of pellet injection on both confinement and ELM behaviour is to seek to identify a physical system whose relaxation processes have characteristics similar to those of the ELMing process under consideration. Of particular interest is the sandpile[16], whose relevance to fusion plasmas is well known[17, 18].

Sandpile models generate avalanches, which may be internal or result in loss of particles from the system. These avalanches are the response to steady fuelling of a system which relaxes through coupled near-neighbour transport events that occur whenever a critical gradient is locally exceeded. The possibility that, in some circumstances, ELMing may resemble avalanching was raised[19] in studies of the specific sandpile model of Ref.[20]. This simple one-dimensional N-cell sandpile model[19, 20] incorporates other established models[16, 21] as limiting cases. It is centrally fuelled at cell $n = 1/500$, and its distinctive feature is the rule for local redistribution of sand near a cell (say at $n = k$) at which the critical gradient *Zc* is exceeded. The sandpile is conservatively flattened around the unstable cell over a fast redistribution lengthscale *Lf*, which spans the cells $n = k - (LF - 1), k - (Lf - 2), \ldots , k+1,$ so that the total amount of sand in the fluidization region before and after the flattening is unchanged. Because the value at cell $n = k+1$ prior to the redistribution is lower than the value of the cells behind it, the redistribution results in the relocation of sand from the fluidization region, to the cell at $n = k + 1$. If redistributions are sequentially triggered outwards across neighbouring cells, leading to sand ultimately being output at the edge of the sandpile, an avalanche is said to have occurred. The sandpile is then fuelled again, either after the sandpile has iterated to stability so that sand ceases to escape from the system (`classic model'), or immediately after the first `sweep' through the system has been completed (`running model').

In the `classic' sandpile model, the avalanche may propagate through the sandpile multiple times until the system ceases to output sand, prior to further fuelling of the sandpile. Effectively, fuelling is paused until the

system is stable, which reflects the instantaneous nature of an avalanche, by comparison to the slow addition of single grains of sand. In the `running model' which was first explored in [22], the sandpile is fuelled again as soon as the first iteration of the avalanche is complete, while the sandpile remains in critical state. In the low fuelling regime, little difference is observed between the classic model and the running model, as the sandpile may take, say, 500 iterations to reach stability, during which time enough sand has been added at the first cell to cause the critical gradient to be exceeded between the first and second cells a further one or two times. Compared to the total amount of sand which may be lost in the continuing avalanche, the further added sand is of little relevance. By comparison, if a high fuelling rate is employed, then the extra sand added during the continuing avalanche becomes significant, and can significantly change the overall behaviour in the running model.

Typically, sandpile models are analysed in the low driving regime, as low driving is considered to be necessary to achieve a separation of time scales which is a condition of SOC [23]. High driving has also been considered in relation to the Chapman model [23, 24] and been found to lead to the elimination of the smallest scale avalanches. Further, an analogy between the Reynolds number, and the relationship between driving and dissipation has been identified and found to give a means of distinguishing between turbulence and SOC[25, 26]. In this study, we have focused on the high discrete driving regime, and its relationship to the total potential energy of the system, and to mass loss events (MLEs).

Here, following [22], we seek to draw comparisons with pellet pacing by varying the amount of sand, *dx*, added at each time step. We do this both by setting a high constant *dx* in order to move into the high fuelling regime, and also by varying *dx* intermittently to seek to trigger avalanches. By doing this, we are able to compare systems where `pellets' are added at each time step before the system has an opportunity to fully relax (using high constant *dx* in the running model), and systems in which the system can fully relax between `pellets', using the classic model at low fuelling with the intermittent addition of `pellets'.

We also briefly comment on the behaviour of the classic model at high fuelling, although our focus is on the behaviour of the running model at high fuelling, and on the introduction of intermittent pellets into the classic model.

The lengthscale *Lf*, normalized to the system scale *N*, is typically [17, 19, 24, 27, 28] treated as the model's primary control parameter *Lf/N*, which governs different regimes of avalanche statistics and system dynamics.

Unlike some implementations of the Chapman model[17, 19, 24, 27, 28], but following [22] and [29], *Zc* is single valued, rather than being randomized. The phenomenology generated by this model has several features resembling tokamak plasmas, including edge pedestals, enhanced confinement[19] and self-generated internal transport barriers[28]. Particularly relevant here are the systemwide avalanches, or MLEs, resulting (unlike the more numerous internal avalanches which are not considered here) in mass loss from the sandpile.

We observe that there is no single relationship between driving, waiting times, and potential energy, which holds in all regimes. Further, the nature of the relationship is different for the classic model and the running model. We comment here on the different relationships in different driving regimes, and offer some suggestions as to the reasons for those relationships, and whether there are real world scenarios which may be informed by those reasons.

2. INTERMITTENT EXTRA SAND

We have taken the classic and running models and added extra sand (pellets) in various combinations of intervals, and pellet size, by way of comparison to pellet pacing in fusion plasmas.

In general, we observe that *Ep* and maximum MLE size move in the same direction (up or down), although maximum MLE size changes more quickly than *Ep*.

For this purpose, there is a close relationship between the high driving regime discussed in section 3 below and the intermittent addition of extra sand. If the extra sand is absorbed into the sandpile without triggering an MLE, then the addition of the extra sand may serve simply to increase fuelling of the system. On the other hand, if the intermittent addition of extra sand triggers an MLE when the extra sand is added, the system may behave quite differently. Three waiting times are considered here - the waiting time between pellets, *Tp*, the 'natural' waiting time between MLEs for a given amount of fuelling (including pellet fuelling), *Tn*, and the actual waiting time

observed, *Ta*. *Tn* and *Ta* will be equal to each other if the pellets do nothing more than add to total fuelling, without triggering a 'shock' to the system which triggers an immediate MLE before the system would otherwise have reached a critical state if the total fuelling had been constant.

Lang [8] discussed pellets added at lower frequencies (higher *Tp*) with pellet timing aligned to ELM onset. These pellets triggered ELMs. Lang[8] observes that as pellets increase the plasma density, this in turn increases the L-H threshold.

We have tested these observations against our model. We observe that while *Ep* increases with pellet size, maximum MLE size also increases, and at a faster rate.

For `macro' pellets, we show here results for two primary waiting times - 70000 and 100000. Short and long *Tn* are typically observed in the model: the 'short' *Tn* for this model with *dx*=1.2 is ~70000, with a longer *Tn* at ~140,000. The values of *Tp* selected therefore represent different stages in build-up approximately at, or post, avalanching (recognizing that the additional fuel added by way of 'pellets' also increases total fueling).

We observe that the size of the maximum MLE is roughly equal to double the amount of material added during the longest waiting time. As a result, if the longest waiting time remains approximately constant while the amount of material added per unit time increases, then the maximum MLE size goes up.

As shown in *FIG. 2*(a), for *Tp*=70000, both potential energy and maximum MLE size increase, although maximum MLE size increases faster, with increasing pellet size. It is apparent that, at least in this model, adding pellets at the core will not reduce MLE size. In order to reach the threshold for triggering MLEs with the addition of each pellet, pellets must be so large that the resulting MLE is of a greater size than 'natural' MLEs, and, further, that fuelling becomes effectively dominated by pellets. As a result, pellet fuelling at the core is not effective to reduce MLE size in this model.

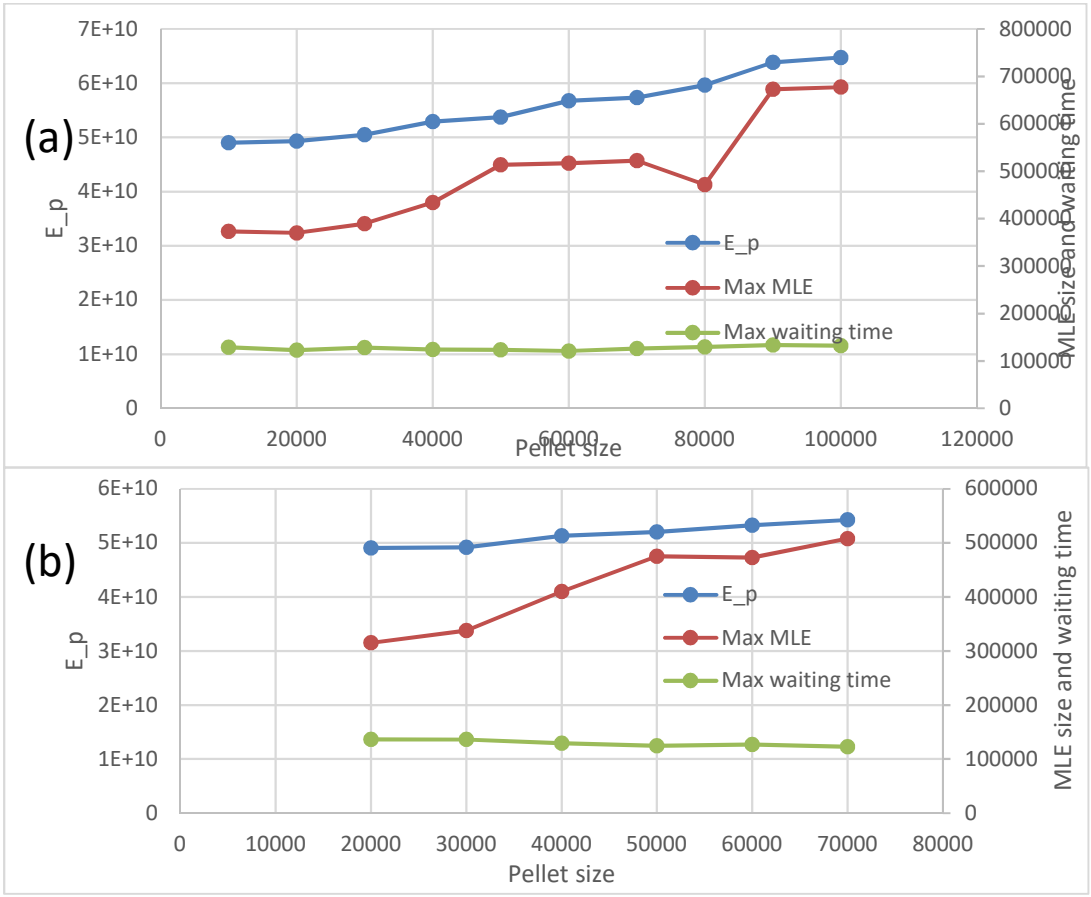

FIG. 1 Variation of Ep, Max MLE, and Max Ta with pellet size. Pellets are added at the core. (a) Tp = 70,000; (b) Tp= 100,000

3. HIGH DRIVING - CONSTANT FUELLING

3.1. Introduction

We now consider the impact of increasing constant fuelling, primarily in the running model. We have also considered increasing constant fuelling in the classic model, in which little effect is seen other than to increase MLE frequency due to the faster build-up of the sandpile.

3.2. *Ep* for classic and running models - low driving

Before commenting on the high driving regimes, we first comment on some relationships observed at low driving, for the purposes of observing the changes in those relationships as driving increases. For all examples, Zc=120, meaning that for dx=1.2, dx/Zc=0.01.

We first consider changes in the driving regime for the classic and running models up to dx = 30. *FIG. 2* shows that the classic and running models produce very similar results in terms of *Ep* up to dx=1.2, but vary significantly above dx=1.2. At its simplest, this variation may be attributed to the amount of fuel added during a continuing avalanche in the running model becoming significant, while the increase in fueling in the classic model does not impact on total system size, but simply on the waiting time between MLEs.

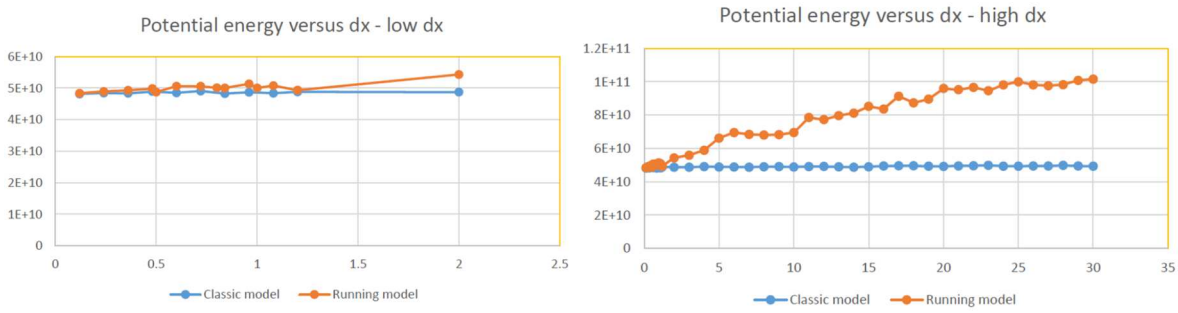

FIG. 2 (a) *Ep* versus dx up to dx = 2, for classic and running models. It is notable that *Ep* is effectively constant for all values of dx shown here in the classic model, while *Ep* gradually increases in the running model. However, the increase in *Ep* for values of dx up to 1.2 is very minor and may only represent noise. (b) *Ep* versus dx up to dx = 30, for classic and running models. It is notable that *Ep* is effectively constant for all values of dx shown here in the classic model, while *Ep* gradually increases in the running model.

3.3. Relationship between driving and potential energy - running model

We now turn to consider the behaviour of the running model at high constant driving. Unlike the classic model, significant changes in behaviour of the system are observed as driving increases in the running model.

We show in *FIG. 3* Ep against dx for four different sets of values of Zc and Lf, for values of dx/Zc up to 1. A clear upward trend is observable as we increase dx/Zc up to about .3, with a subsequent general decline, subject to significant detailed structure.

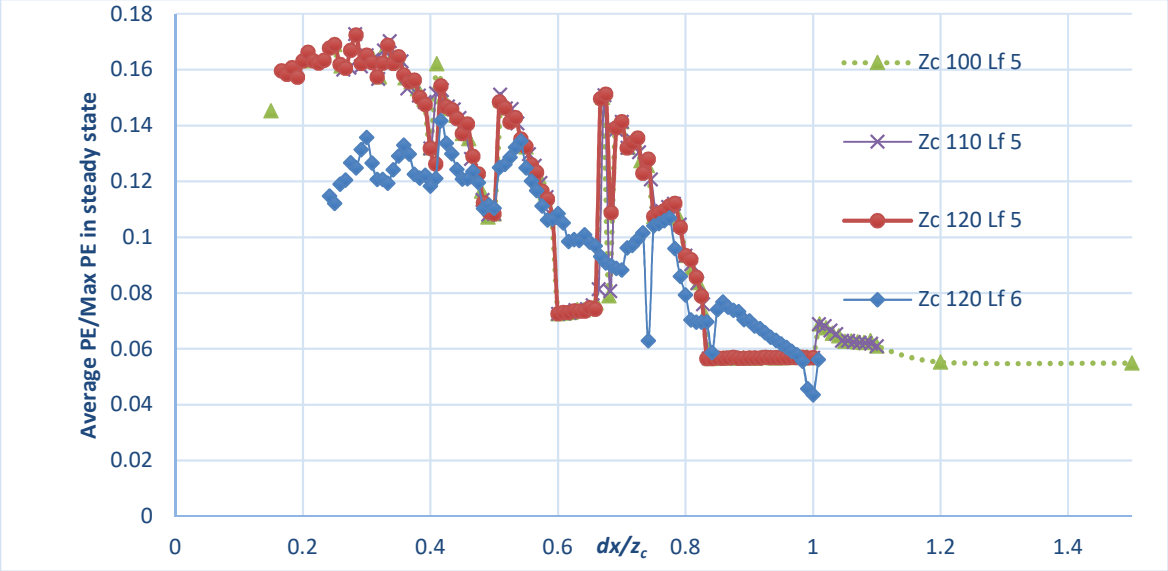

FIG. 3 Potential energy/Maximum potential energy vs dx/Zc (all unitless). The potential energy measured is the average potential energy (given by the sum of the squares of the cells) after the system has evolved from a nil sandpile to a 'steady state', which typically takes several hundred thousand iterations. The three curves which largely coincide represent data for different values of Zc, but common values of Lf. The other curve represents data for a changed value of Lf. It is notable that fine structure is seen around integer ratios of dx/Zc

We first comment on the upwards trend, before commenting on the detailed structure. The primary peak is situated at approximately *dx*/*Zc*=0.3, which is to say that the energy of the sandpile is maximised if the amount of sand added at each timestep is about 1/3 of that sufficient to provoke an avalanche (assuming an otherwise nil gradient at the top of the sandpile). In most cases, the avalanche will not be systemwide, but will terminate before it reaches the edge.

FIG. 3 demonstrates that the fine structure relates to integer ratios of *dx*/Zc. Further, the shape of this potential energy curve is unchanged with variations in *Zc*, although it is not constant with changes in *Lf*. We also observe that while all significant changes appear to correspond with integer ratios, not all integer ratios correspond with significant changes.

A qualitative explanation for this behaviour may be suggested as follows. As demonstrated in *FIG. 4*, the amount of sand to be distributed at each time step will increase as *dx* increases, but will decrease just at or after integer ratios of *dx*/Zc. In *FIG. 4*(a), where *dx* exceeds *Zc* by a small amount, only a single unit of *dx* is to be distributed at each timestep. In *FIG. 4*(b), where *Zc* exceeds *dx* by a small amount, two units of *dx* are distributed in each avalanche, approximately at every second timestep.

In a particular example, the point at which the amount of sand to be distributed increases or decreases will also be dependent upon the actual gradient of the sandpile at that time. Although the sandpile may have a non-zero average gradient, it will nonetheless commonly be the case that adjoining cells take on identical values, as a result of avalanches which have not caused the critical gradient to be exceeded at all cells, even though they may have propagated entirely through the sandpile. From the perspective of such adjoining cells, the total amount of sand added to the system may result in the critical gradient being exceeded at those points, even though the sum of the average gradient and *dx* is greater than the critical gradient at other points in the sandpile. The closer the actual gradient to the critical gradient following an avalanche, the lesser the amount of sand which must be added to trigger the following avalanche. The larger the amount of sand to be redistributed in a particular avalanche, the less likely it is that the sand will be assimilated within the sandpile, rather than causing a systemwide avalanche[23].

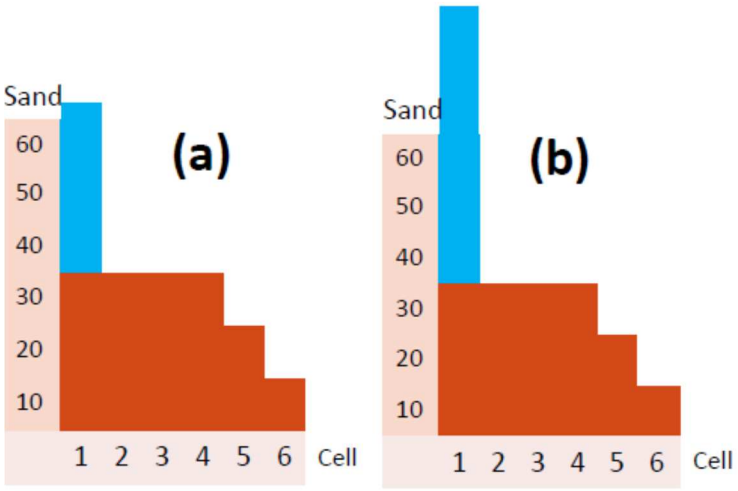

FIG. 4 (a) dx=32, Zc =30. One iteration enough for gradient to exceed Zc. 32 grains to be distributed.(b) dx=29, Zc =30. Two iterations required for gradient to exceed Zc. 58 grains to be distributed.

Regardless of whether or not the integer ratio behaviour observed in the potential energy curve is repeated in other sandpile models, this heuristic explanation suggests that the behaviour may be observable in real world scenarios involving large discrete fuelling. In particular, this behaviour may be observed in fuelling of a fusion plasma by pellet injection.

4. CONCLUSIONS

These observations may be summarized as follows:

a) Addition of pellets at the core results in an increase in *Ep* in the system, but also results in larger MLEs, suggesting that the addition of pellets at the core is not effective for MLE (or ELM) reduction;
b) At low *dx*, *Ep* varies with *dx* in the running model, while *Ep* remains constant in the classic model;
c) Waiting times scale inversely with fuelling in the classic model, consistent with the observation that *Ep* is unchanged, such that MLEs depend on the amount of sand in the system, and not on the rate at which the sand builds up
d) Comparing *Ep*/*Ep max* against *dx*/*Zc* for increasing *dx* shows that step changes occur, often at integer ratios. An heuristic explanation is suggested for this behaviour

ACKNOWLEDGMENTS

This work was jointly funded by the Australian Research Council through grant FT0991899 and the Australian National University. One of the authors, C. A. Bowie, is supported through an ANU PhD scholarship, an Australian Government Research Training Program (RTP) Scholarship, and an Australian Institute of Nuclear Science and Engineering Postgraduate Research Award.

[1] Hong W Y, Wang E Y, Pan Y D and Xu X Q 1999 Effects of supersonic beam and pellet injection on edge electric field and plasma rotation in {HL-1M} *Journal of Nuclear Materials* **266** 542-5
[2] Baylor L R, Jernigan T C, Burrell K H, Combs S K, Doyle E J, Gohil P, Greenfield C M, Lasnier C J and West W P 2005 Fueling of {QH}-mode plasmas on {DIII-D} with pellets and gas *Journal of Nuclear Materials* **337** 535-8
[3] Baylor L R, Parks P B, Jernigan T C, Caughman J B, Combs S K, Foust C R, Houlberg W A, Maruyama S and Rasmussen D A 2007 Pellet fuelling and control of burning plasmas in {ITER} *Nuclear Fusion* **47** 443
[4] Baylor L R, Commaux N, Jernigan T C, Brooks N H, Combs S K, Evans T E, Fenstermacher M E, Isler R C, Lasnier C J, Meitner S J, Moyer R A, Osborne T H, Parks P B, Snyder P B, Strait E J, Unterberg E A and Loarte A 2013 Reduction of {E}dge-{L}ocalized {M}ode Intensity Using High-Repetition-Rate Pellet Injection in {T}okamak {H}-{M}ode Plasmas *Physical Review Letters* **110** 245001
[5] Baylor L R, Lang P T, Allen S L, Combs S K, Commaux N, Evans T E, Fenstermacher M E, Huijsmans G, Jernigan T C, Lasnier C J, Leonard A W, Loarte A, Maingi R, Maruyama S, Meitner S J,

Moyer R A and Osborne T H 2015 {ELM} mitigation with pellet {ELM} triggering and implications for {PFC}s and plasma performance in {ITER} *Journal of Nuclear Materials* **463** 104-8

[6] Lang P T, Conway G D, Eich T, Fattorini L, Gruber O, Gunter S, Horton L D, Kalvin S, Kallenbach A, Kaufmann M, Kocsis G, Lorenz A, Manso M E, Maraschek M, Mertens V, Neuhauser J, Nunes I, Schneider W, Suttrop W, Urano H and {ASDEX Upgrade Team} 2004 {ELM} pace making and mitigation by pellet injection in {ASDEX} {U}pgrade *Nuclear Fusion* **44** 665-77

[7] Lang P T, Burckhart A, Bernert M, Casali L, Fischer R, Kardaun O, Kocsis G, Maraschek M, Mlynek A, Plöckl B, Reich M, Ryter F, Schweinzer J, Sieglin B, Suttrop W, Szepesi T, Tardini G, Wolfrum E, Zasche D, Zohm H and Team A U 2014 {ELM} pacing and high-density operation using pellet injection in the {ASDEX} {U}pgrade all-metal-wall tokamak *Nuclear Fusion* **54** 083009

[8] Lang P T, Meyer H, Birkenmeier G, Burckhart A, Carvalho I S, Delabie E, Frassinetti L, Huijsmans G, Kocsis G, Loarte A, Maggi C F, Maraschek M, Ploeckl B, Rimini F, Ryter F, Saarelma S, Szepesi T, Wolfrum E, Team A U and Contributors J E T 2015 ELM control at the L → H transition by means of pellet pacing in the ASDEX Upgrade and JET all-metal-wall tokamaks *Plasma Physics and Controlled Fusion* **57** 045011

[9] Pegourie B 2007 Review: Pellet injection experiments and modelling *Plasma Physics and Controlled Fusion* **49** R87-R160

[10] Rhee T, Kwon J M, Diamond P H and Xiao W W 2012 On the mechanism for edge localized mode mitigation by supersonic molecular beam injection *Physics of Plasmas* **19** 022505

[11] Lang P T, Blanken T C, Dunne M, McDermott R M, Wolfrum E, Bobkov V, Felici F, Fischer R, Janky F, Kallenbach A, Kardaun O, Kudlacek O, Mertens V, Mlynek A, Ploeckl B, Stober J K, Treutterer W, Zohm H and {ASDEX Upgrade Team} 2018 Feedback controlled, reactor relevant, high-density, high-confinement scenarios at {ASDEX} {U}pgrade *Nuclear Fusion* **58** 036001

[12] Lang P T, Alonso A, Alper B, Belonohy E, Boboc A, Devaux S, Eich T, Frigione D, Gál K, Garzotti L, Geraud A, Kocsis G, K{ö}chl F, Lackner K, Loarte A, Lomas P J, Maraschek M, M{ü}ller H W, Neu R, Neuhauser J, Petravich G, Saibene G, Schweinzer J, Thomsen H, Tsalas M, Wenninger R, Zohm H and {JET EFDA Contributors} 2011 {ELM} pacing investigations at {JET} with the new pellet launcher *Nuclear Fusion* **51** 033010

[13] Li C, Hu J, Chen Y, Liang Y, Li J, Li J, Wu J and Han X 2014 First Results of Pellet Injection Experiments on {EAST} *Plasma Science and Technology* **16** 913

[14] Yao X J, Hu J S, Chen Y, Sun Z, Liu H Q, Lian H, Wang S X, Jie Y X, Shi N, Xu G S, Yang Q Q, Shi T H, Zhou C, Xu Z, Zhu X, Wang T F, Zang Q, Yuan Y, Li C Z, Zhen X W, Gong X Z, Li J, Wu G J, Yuan X L and {The EAST Team} 2017 {H}-mode achieved by pellet injection in experimental advanced superconducting tokamak *Nuclear Fusion* **57** 066002

[15] Doyle E J, Houlberg W A, Kamada Y, Mukhovatov V, Osborne T H, Polevoi A, Bateman G, Connor J W, Cordey J G, Fujita T, Garbet X, Hahm T S, Horton L D, Hubbard A E, Imbeaux F, Jenko F, Kinsey J E, Kishimoto Y, Li J, Luce T C, Martin Y, Ossipenko M, Parail V, Peeters A, Rhodes T L, Rice J E, Roach C M, Rozhansky V, Ryter F, Saibene G, Sartori R, Sips A C C, Snipes J A, Sugihara M, Synakowski E J, Takenaga H, Takizuka T, Thomsen K, Wade M R, Wilson H R, {ITPA Transport Phys Topical Group}, {ITPA Confinement Database Modelling Topical Group} and {ITPA Pedestal Edge Topical Group} 2007 Chapter 2: Plasma confinement and transport *Nuclear Fusion* **47** S18-S127

[16] Bak P, Tang C and Wiesenfeld K 1987 Self-Organized Criticality - An Explanation of 1/f Noise *Physical Review Letters* **59** 381

[17] Chapman S C, Dendy R O and Rowlands G 1999 A sandpile model with dual scaling regimes for laboratory, space and astrophysical plasmas *Physics of Plasmas* **6** 4169-77

[18] Dendy R O and Helander P 1997 Sandpiles, silos and tokamak phenomenology: a brief review *Plasma Physics and Controlled Fusion* **39** 1947-61

[19] Chapman S C, Dendy R O and Hnat B 2001 Sandpile model with tokamaklike enhanced confinement phenomenology *Physical Review Letters* **86** 2814-7

[20] Chapman S C 2000 Inverse cascade avalanche model with limit cycle exhibiting period doubling, intermittency, and self-similarity *Physical Review E* **62** 1905-11

[21] Dendy R O and Helander P 1998 Appearance and nonappearance of self-organized criticality in sandpiles *Physical Review E* **57** 3641-4

[22] Bowie C A, Dendy R O and Hole M J 2016 Delay time embedding of mass loss avalanches in a fusion plasma-oriented sandpile model *Physics of Plasmas* **23** 100703

[23] Watkins N W, Chapman S C, Dendy R O and Rowlands G 1999 Robustness of collective behaviour in strongly driven avalanche models: Magnetospheric implications *Geophysical Research Letters* **26** 2617-20

[24] Chapman S C, Dendy R O and Watkins N W 2004 Robustness and scaling: key observables in the complex dynamic magnetosphere *Plasma Physics and Controlled Fusion* **46** B157-B66

[25] Chapman S C and Watkins N W 2009 Avalanching systems under intermediate driving rate *Plasma Physics and Controlled Fusion* **51** 9
[26] Chapman S C, Rowlands G and Watkins N W 2009 Macroscopic control parameter for avalanche models for bursty transport *Physics of Plasmas* **16**
[27] Chapman S C, Dendy R O and Hnat B 2001 A simple avalanche model for astroplasma and laboratory confinement systems *Physics of Plasmas* **8** 1969-76
[28] Chapman S C, Dendy R O and Hnat B 2003 Self-organization of internal pedestals in a sandpile *Plasma Physics and Controlled Fusion* **45** 301
[29] Bowie C A and Hole M J 2018 Pedestals and feedback in fusion-plasma relevant sandpile models *Physics of Plasmas* **25** 012511